Pure Appl. Geophys. 172 (2015), 3385–3407

DOI 10.1007/s00024-015-1136-4

Pure and Applied Geophysics

Tsunami Impact Computed from Offshore Modeling and Coastal Amplification Laws: Insights from the 2004 Indian Ocean Tsunami

H. Hébert[1] and F. Schindelé[1]

Abstract—The 2004 Indian Ocean tsunami gave the opportunity to gather unprecedented tsunami observation databases for various coastlines. We present here an analysis of such databases gathered for 3 coastlines, among the most impacted in 2004 in the intermediate- and far field: Thailand–Myanmar, SE India–Sri Lanka, and SE Madagascar. Non-linear shallow water tsunami modeling performed on a single 4′ coarse bathymetric grid is compared to these observations, in order to check to which extent a simple approach based on the usual energy conservation laws (either Green's or Synolakis laws) can explain the data. The idea is to fit tsunami data with numerical modeling carried out without any refined coastal bathymetry/topography. To this end several parameters are discussed, namely the bathymetric depth to which model results must be extrapolated (using the Green's law), or the mean bathymetric slope to consider near the studied coast (when using the Synolakis law). Using extrapolation depths from 1 to 10 m generally allows a good fit; however, a 0.1 m is required for some others, especially in the far field (Madagascar) possibly due to enhanced numerical dispersion. Such a method also allows describing the tsunami impact variability along a given coastline. Then, using a series of scenarios, we propose a preliminary statistical assessment of tsunami impact for a given earthquake magnitude along the Indonesian subduction. Conversely, the sources mostly contributing to a specific hazard can also be mapped onto the sources, providing a first order definition of which sources are threatening the 3 studied coastlines.

Key words: Tsunamis, Indian Ocean, numerical modeling, nearshore processes, subduction zones.

1. Introduction

The 2004 great, catastrophic tsunami in the Indian Ocean has underlined the threat posed by major transoceanic tsunamis in this specific ocean, where the available historical catalogs were probably not thoroughly representative to assess the actual hazard, although historical transoceanic tsunamis were known in the area (e.g. 1881 in the Nicobar Islands) (Ortiz and Bilham 2003). Actually most of the major 20th century tsunamis had previously occurred in the Pacific Ocean (1946, 1960) (Gusiakov 2005), a basin where similar destructive events can occur several times a century. The extent of the 2004 tsunami aftermath urged the need for a better assessment of tsunami hazard not only in the Indian Ocean, but also for every oceanic basin especially in terms of designing and deciding the establishment of new warning systems. Since tsunami hazard assessment essentially relies on historical databases completed by numerical modeling (Synolakis and Bernard 2006), the opportunity to test the methods against the unprecedented 2004 databases and also to propose original methodologies had to be stressed.

Numerous numerical modelings of this tsunami have been proposed, to determine the source characteristics (e.g. Fuji and Satake 2007; Sladen and Hébert 2008; Lorito *et al.* 2010), or the response of various coastal sites at local more detailed level (Hébert *et al.* 2007; Poisson *et al.* 2009) or at a regional level (Ioualalen *et al.* 2007). The extent of the event also gave the opportunity to initiate reflections on tsunami hazard and forecasting techniques (Geist *et al.* 2007), and to launch new warning system architectures in every ocean deprived of, in priority in the Indian Ocean (e.g. Rudloff *et al.* 2009 and papers therein) and also in the Mediterranean Sea (Tinti *et al.* 2012; Schindelé *et al.* 2015).

Detailed hazard mapping, an approach which is still demanding in terms of involved models, data and uncertainties, was already performed by various authors (Yanagisawa *et al.* 2009; Okal and

[1] CEA, DAM, DIF, 91297 Arpajon, France. E-mail: francois.schindele@gmail.com; helene.hebert@cea.fr

Synolakis 2008) for selected sites in the Indian Ocean. We aim here at taking advantage of the large amount of unique observation data available after the 2004 tsunami to test the efficiency of the modeling methods, and to discuss some of the characteristics of the non-linear nearshore tsunami amplification. Simple approaches are indeed available to rapidly assess a tsunami impact for a given coastal site, using empirical amplification laws, without conducting detailed, computationally costly modeling. This kind of approach needs being validated against actual data sets, nowadays when, more than 10 years after the 2004 catastrophe and following the 2011 catastrophic tsunami in the Pacific, they are more and more used in the operational frames of warning centers (Reymond *et al.* 2012).

We study the 2004 tsunami using detailed data available on different sites (Thailand–Myanmar, Sri Lanka and Madagascar, see location on Fig. 1), located at different distances from the earthquake epicentral area, and we compare these observations with numerical modeling results performed on coarse grids without any bathymetric refinement. To this end we test tsunami amplification laws that provide good approximations for the tsunami shoaling effect in the shallowest portion of the ocean. This method allows proposing average trends for the tsunami impacts on a given shoreline that can be quickly computed, explain a major part of the observed damage in 2004, and help to assess tsunami hazard in real time.

2. Context and Objectives

The most devastating tsunamis at regional scales are due to earthquakes, and are able to propagate damaging energy at far distances, because of the long wavelengths implied. They are usually triggered by the largest submarine quakes, mostly the thrusting events occurring on well-known subduction zones. However, in many oceanic basins, tsunami catalogs reflect a heterogeneous database that may be poorly

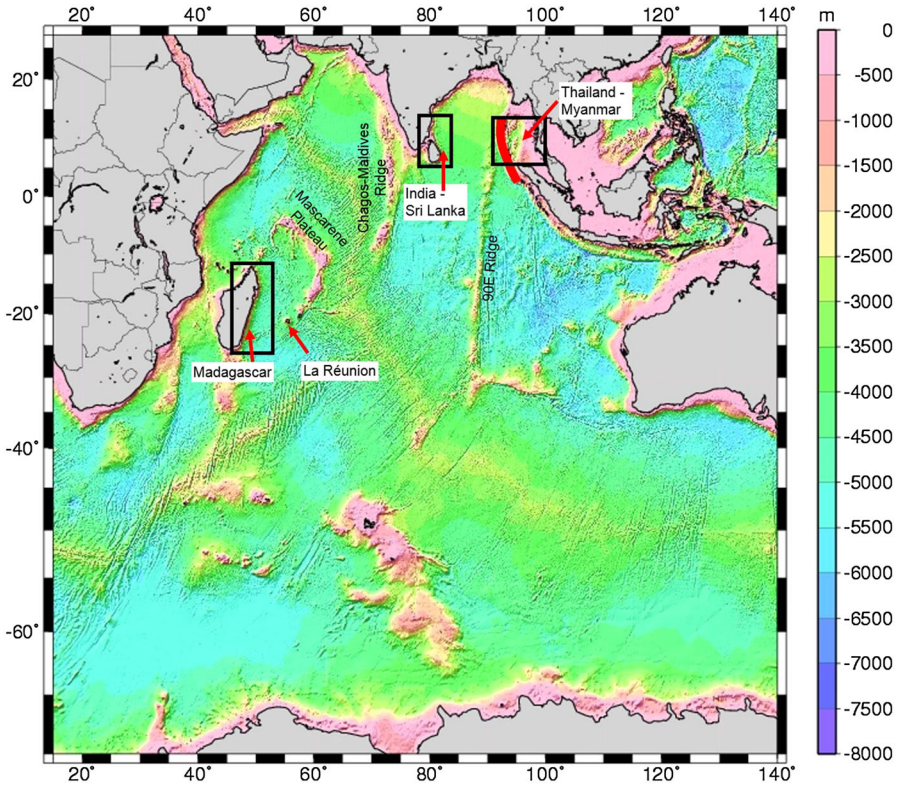

Figure 1
Bathymetric grid describing the Indian Ocean at a 4′ cell size, and location of the 3 coastal regions of this study. The *thick red line* indicates the coseismic area of the 26 December 2004 earthquake

representative for the recent tsunami history. For instance, the Mediterranean Sea is well known for key historical events, especially in its eastern region (large tsunamis due to rare, large earthquakes in Crete, or cataclysmic volcanic explosion in Santorini) (Soloviev *et al.* 2000), as is the NE Atlantic Ocean (1755 tsunami off Lisbon) (Baptista *et al.* 2003). Recent events, often more moderate (Baptista and Miranda 2009), tend to underestimate the actual tsunami hazard in most of those areas. Similarly in the Indian Ocean, destructive events were not to be discarded (Ortiz and Bilham 2003), even though the extent of the 2004 earthquake and tsunami was honestly not foreseen by the geophysicists. The same remarks also apply to the Tohoku area where the expected magnitude was much lower than the event actually triggered in 2011, although historical and geological evidences could have favored such scenarios (Sawai *et al.* 2012).

The 2004 tsunami belongs to the category of events related to subduction processes, whose return periods are quite long (above 500 year), and which give rise to large tsunamis every 500–700 year at least (Jankaew *et al.* 2008). The historical seismic activity of the Sunda Arc (Zachariasen *et al.* 1999; Subarya *et al.* 2006) indicates that important tsunamis may have repeatedly occurred there. The relative regional quiescence during the 20th century together with the poor amount of earlier observations among the Indian Ocean residents was not in favor of a proper awareness of tsunami hazard along the coasts facing this ocean.

In addition to historical catalogs, tsunami hazard studies can rely on paleotsunami investigation on well-preserved paleoshoreline environments, and on numerical modeling whose recent advances allowed refining the quantitative results in terms of tsunami heights, flooding areas characteristics, and also toward the assessment of damage on buildings and facilities (Synolakis 2002). Tsunami numerical modeling, as for every natural phenomenon, can illustrate every sequence of the process, including all uncertainties therein (Synolakis and Bernard 2006).

Three major steps can be defined: the initiation, the deep sea propagation, and the coastal amplification (where the tsunami is actually observed and causes damage). While the offshore propagation can be easily modeled through the simple approximation of the shallow water equations, the source and coastal processes often remain delicate to be numerically handled. As for the initiation, usual elastic dislocation models (e.g. Okada 1985) provide a good approximation for the initial static coseismic triggering. The limitation here mostly consists of uncertainties on the seismological parameters used for the earthquake source. On the coasts, the limitations arise not only on the parameters to be used, namely the resolution of the bathymetric grids and the extent of the topographic data available, but also on the models used. A non-linear shallow water model is usually used, including non-linear terms to properly take into account the amplifying shoaling effect. However, the validity of such models appears more questionable for very high, short tsunami waves that interact with strong discontinuities (cliffs, buildings) and/or with various ground morphologies that can also be expressed in terms of various bottom friction coefficients. Indeed for instance, including variable friction coefficients in the shallowest bathymetry, following a Chezy approach, significantly modifies amplitudes of synthetic tide gauges (example in the Pacific Ocean, e.g. Hébert *et al.* 2009).

In the following study of the 2004 tsunami, we test a couple of amplification laws among those known in the literature. We avoid intensive modeling in the coastal areas, but provide instead a first order approximation of the tsunami heights that can be rapidly computed. Since these amplification laws implicitly contain the specific characteristics of the coastal response, and also depend on the coarse models performed, they have to be fit for each region studied. Then we attempt to propose a statistical approach to the coastal tsunami hazard, for several earthquake scenarios of a given magnitude along the Java–Sumatra trench. This allows to underline some specific regions as more prone to tsunami amplifications, for a given selection of scenarios.

3. Methods and Data

3.1. Tsunami Numerical Modeling

As explained above, the tsunami source is usually treated as an instantaneous perturbation of the sea bottom in response to the static displacement due to the earthquake. The initial deformation is computed here

through a model of elastic dislocation (Okada 1985) constrained with seismological parameters of the rupture that satisfy the expression of moment magnitude $M_0 = \mu ULW$, where μ is the rigidity, U the average slip amount and L (W) the length (width) of the fault plane (e.g. Kanamori and Anderson 1975). Such seismological parameters describing the fault geometry are mostly obtained from the inversion studies available when large earthquakes occur, or they are adapted from regional realistic seismotectonics, when various scenarios must be defined.

The modeling of tsunami propagation is carried out using algorithms solving the hydrodynamic equations under the non-linear shallow water theory. Equations of continuity (1) and motion (2) are here solved in spherical coordinates by means of a finite-difference method, centered in time, and using an upwind scheme in space (Heinrich *et al.* 1998; Hébert *et al.* 2001). Open free boundary conditions are ascribed to the grid boundaries.

$$\frac{\partial(\eta + d)}{\partial t} + \nabla \times [\mathbf{v}(\eta + d)] = 0 \qquad (1)$$

$$\frac{\partial(\mathbf{v})}{\partial t} + (\mathbf{v} \times \nabla)\mathbf{v} = -\mathbf{g}\nabla\eta \qquad (2)$$

where d is the sea depth, η is the water elevation above mean sea level, $\mathbf{v}$ is the depth-averaged horizontal velocity vector, and $\mathbf{g}$ is the gravitational acceleration. The time increment Δt is constrained by the Courant–Friedrichs–Lewy criterion imposing $\Delta t \ll \Delta x/\sqrt{gh}$ where Δx is the space increment. To properly handle the shoaling effect near the coasts, refined grids, or nested bathymetric grids with increasing resolution, should be used to describe the refinement of bathymetric features when the water depth h decreases, hence when the tsunami wavelengths shorten, as well as the coastal structures. The method also allows to compute the inundation onshore provided topographic high resolution data are available. In the following, where only a coarse approach is tested, neither grid refinement and nesting, nor onshore run-up computations are performed.

3.2. Bathymetric Data

The computational domain relies on bathymetric data describing the sea depth d at each grid point. Usually coarse modeling is performed using bathymetric data from public datasets, such as the one derived from satellite altimetry (ETOPO2 bathymetric, 2′ grid cell size) (Smith and Sandwell 1997), or the oceanographic synthesis GEBCO (1′ grid cell) (GEBCO 2006). For this study, a bathymetric grid derived from ETOPO2 has been built in order to encompass the source area as well as the targets to be studied (Fig. 1). In order to reduce the computational time and increase the number of tests, the grid has been resampled to a 4′ cell size. In any case, such a grid should allow relative comparisons and also account for the amplification due to significant bathymetric discontinuities such as submarine ridges.

3.3. The Earthquake Sources

The amplification laws can be tested and compared with observations gathered after the 2004 tsunami. To this end, we used two different sources for the Sumatra–Andaman earthquake (Fig. 2). First, a simplified heterogeneous seismological source (model A) describing the 2004 earthquake was set up (Table 1) and successfully tested in detailed modeling for the far field, namely to discuss the impact in La Réunion island (Hébert *et al.* 2007). Second, a homogeneous source accounting for the same seismic moment has been defined, with a uniform slip all along the fault, as it may be defined in the minutes following the earthquake (model B).

For both used sources, the fault geometry consists of 6 segments characterized by fault slips ranging from 3 to 16 m, yielding a maximum positive seafloor displacement of 7 m, in the heterogeneous case, and with a uniform slip of 8.5 m for all subfaults in the homogeneous case (maximum seafloor deformation is then 4 m). The strike follows the mean trench azimuth, while the dip angle is between 12° and 15° from South to North. The fault width is 130 km, and the depth of the center is 20 km. The seismic moment is 6.75×10^{22} Nm, equivalent to $M_w = 9.2$.

3.4. Coastal Amplification Laws

The amplification of tsunamis close to the shores can be described using the law proposed by Green (1837) which predicts that the quantity $\eta d^{1/4}$ remains

constant (see definitions for η and d in Sect. 3.1), due to conservation of the wave energy. This implies that the run-up, if equivalent to η_{max} taken at the water depth d_0, obeys $\eta_{max} \times d_0^{1/4} = \eta \times d^{1/4}$, or $\eta_{max} = \eta\ (d/d_0)^{1/4}$. Such an approach obviously provides an approximation of the wave height as close as possible to the shore, but not of the actual run-up which is theoretically measured at the maximum inundation line.

This kind of law was also extended using a description of the run-up of linear solitary waves (Synolakis 1991; Synolakis and Skjelbreia 1993; Synolakis and Bernard 2006) which interestingly accounts for the mean bathymetric slope β:

$$\frac{R}{d} = 2.831 \sqrt{\cot \beta} \left(\frac{\eta}{d}\right)^{5/4}$$

where R is the maximum run-up. In that case, the value of the mean slope β of the last emerged meters must be estimated, and may much influence the values of the run-up. This law was actually further revised and adapted to work on different waveforms, for instance using N waves, allowing distinguishing leading elevation or depression waves (Tadepalli and Synolakis 1996). Other laws also take into account periodic waves (Pelinovsky and Mazova 1992) and would also deserve to be used against the 2004 database.

In the following, we apply only two laws to the results of coarse tsunami modeling. While the Green's law is widely used as a simple formulation of conservation of energy, the Synolakis law used here should apply only to non-breaking solitary waves. However, although designed for non-breaking solitary waves, a theoretical law such as the one by Tadepalli and Synolakis (1996) actually helped to better understand how, in 2004, the leading depression (toward the eastern Indian Ocean, hence Thailand) implied an increased run-up on average, compared to the leading elevation (toward the western Indian Ocean) (Synolakis and Bernard 2006). The use of the original Synolakis law should be only considered here as a comparison with the Green's law, bearing in mind that many limitations remain when applied to actual tsunami data.

In this study, the basic idea is to retrieve the tsunami heights computed on coarse grids, taken along given bathymetric contours (typically within the last 200–50 m water depths), and then to find the proper shallow water depth to which the tsunami height can be extrapolated, depending on the studied site.

Such an extrapolation approach is used for first order tsunami amplitude assessment. The Japanese Meteorological Agency applies an extrapolation to the water depth of 1 m to assess the expected tsunami heights. It was also applied for tsunami hazard assessment based on near field sources, for instance in South Italy, where the coastal tsunami height can then be easily estimated with a simplified Synolakis law, expressing the mean submarine slope $\cot(\beta)$ by the ratio between the horizontal slope L and the water depth d at the source (Tinti *et al.* 2005). It is worth noting that more recently a probabilistic study involving amplification laws (Green's law; Pelinovsky and Mazova 1992) was conducted to assess the tsunami hazard for the Pacific coastline in central America (Brizuela *et al.* 2014).

4. Application to Several 2004 Tsunami Observation Databases

4.1. Synthesis of Available Data for the 2004 Tsunami for Various Coastal Sites

The 2004 tsunami in the Indian Ocean provided detailed and comprehensive databases of tsunami observations in various coastal contexts, in the near field as in the far field, along linear shorelines as around islands. The tsunami databases usually contain the descriptions of the tsunami arrival, of the water heights, of the run-up heights and the flow depths (IOC 2013), and of the horizontal inundation lengths. Flow depths (within the inundated area) and run-up values (measured inland at the farthest inundation point) should be cautiously distinguished since they are not measured at the same point: a run-up can, for instance, be lower than flow depths at other points on the inundated area, especially when the impacted surface is very flat. This is the case in many 2004 databases, where very low coastal areas produced run-up values smaller than the flow depths over the inundated area (Lavigne *et al.* 2009; Borrero *et al.* 2006).

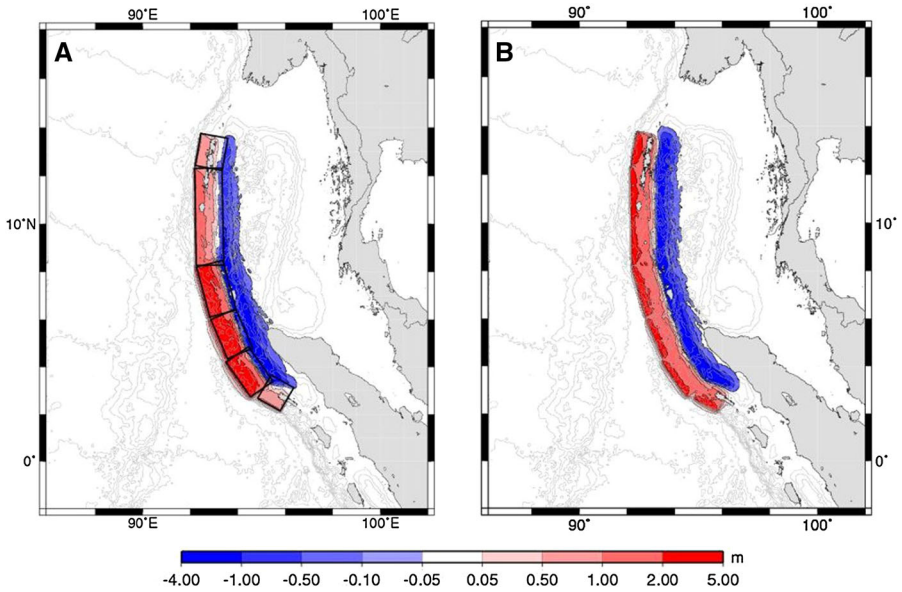

Figure 2
Initial seafloor vertical displacement due to the 2004 earthquake, heterogeneous (**a**), and homogeneous (**b**). Parameters are described in Table 1

Table 1

Parameters of the subfaults used to model the elastic dislocation for the Sumatra earthquake for models A (heterogeneous slip) and B (homogeneous slip)

Subfault	Longitude °E	Latitude °N	Slip (m) Model A	Slip (m) Model B	Strike, dip, rake (°)	Length (km)
1	92.9	13.0	3	8.5	10, 15, 100	150
2	92.8	10.3	5	8.5	359, 14, 98	450
3	93.1	7.3	12	8.5	345, 13, 95	240
4	93.75	5.4	16	8.5	337, 12, 92	200
5	94.5	3.8	12	8.5	325, 12, 92	200
6	95.6	2.9	3	8.5	300, 12, 92	120

The location (longitude and latitude) refers to the central point of the subfault. The central depth is 20 km, the fault width is 130 km throughout the rupture, and the rigidity is fixed to 45 GPa. This model is consistent with a seismic moment of 6.76×10^{22} Nm, or a magnitude M_w 9.16

4.2. Application to Thailand–Myanmar

4.2.1 Observations of the 2004 Tsunami

Thailand coastlines have been heavily affected by the 2004 tsunami, 2 h after the mainshock, and leading to about 8000 casualties among local residents, and on very touristic places. A huge amount of direct observations was besides taken by tourists in pictures, videos, where the catastrophic tsunami impact and energy are well shown. Post-event surveys have been organized to measure the tsunami heights, as early as January 2005, and have confirmed extreme values amounting to 20 m near Khao Lak especially (Tsuji *et al.* 2005, 2006) (Fig. 3). Only a few run-up values are available, most of the measurements consist of tsunami flow depths (tsunami heights inland close to the shore).

By contrast, Myanmar, although located to the close northern vicinity of Thailand, has been much less affected, although the tide level was high (Satake *et al.* 2006), and tsunami heights did not exceed 3 m here. Using an earthquake source not extending northwards to latitude 9°N, as in the first source models following the 26 December mainshock, was a possible explanation for these

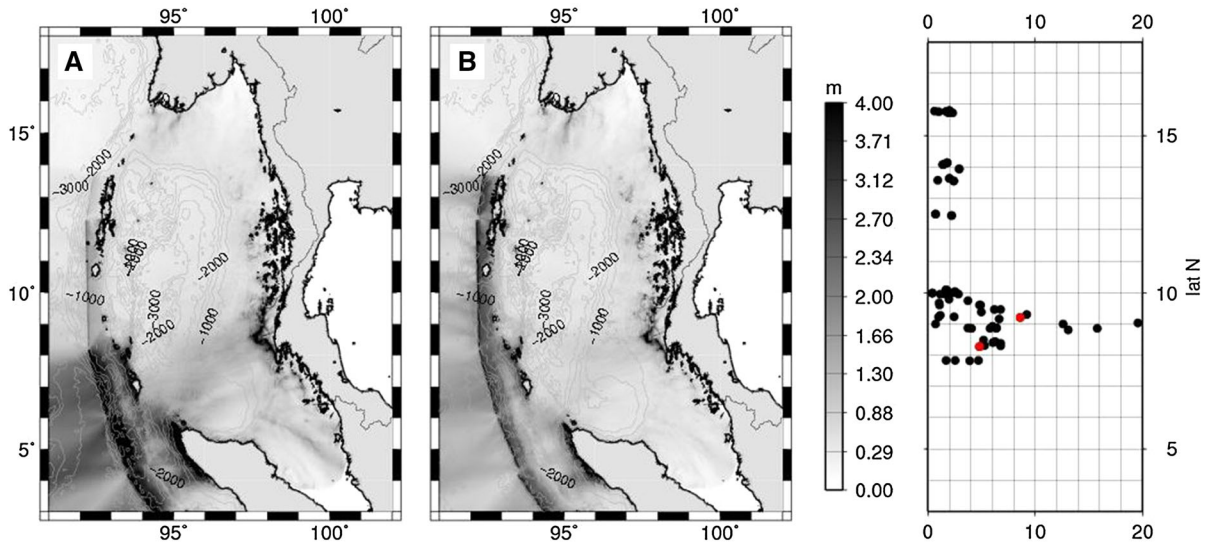

Figure 3
Maximum sea elevations from the heterogeneous (**a**) and homogeneous (**b**) models, after 4 h of propagation, also displaying several annotated bathymetric contours. *Right* tsunami heights measured along the Thailand (south to latitude 10°N) and Myanmar (north to 10°N) coastlines. The *red dots* stand for measured run-up values compared to measured tsunami heights (*black dots*)

contrasting amplitudes (SATAKE *et al.* 2006), but also the protection from offshore islands, and the different bathymetric slopes off Thailand and Myanmar, may be put forward.

4.2.2 *Estimation of Tsunami Heights Using the Green's Law*

Using both source models described above, we apply the Green's law to the Thailand and Myanmar coastlines (Fig. 4a, b). We modeled water heights along 3 bathymetric contours offshore (−200, −100 and −50 m), using the coarse bathymetric grid presented above (results plotted along the different blue colors on Fig. 4). Then the values extrapolated to a given water depth d_0 close to the shore (−10, −1 and −0.1 m) are computed following the dependence on $h^{-1/4}$, for each original deep bathymetry. For a given extrapolation depth d_0 (−10, −1 and −0.1 m), the obtained values for the 3 bathymetric contours are very close, their mean deviation being much smaller than the variations arising from the various extrapolation depths d_0. The values obtained for the 3 deep bathymetric contours are thus averaged to yield a mean profile for a given depth of extrapolation d_0 (various gray lines on Fig. 4).

In practice, for the heterogeneous 2004 source (Fig. 4b), the values computed along the deep bathymetric profiles (in blue) amount to 2–6 m at most, with a maximum clearly evidenced near the value of 360 km (x-axis on Fig. 4), or close to the 9°N latitude (as seen in Fig. 3). When extrapolated to the various shallow water depths d_0 (plotted along the different gray lines) the obtained profiles still exhibit a maximum near this 9°N latitude, where the maximum observations were indeed reported, in the region of Khao Lak. For a depth of extrapolation of −0.1 m, the maximum values reach about 20–24 m, at the location of the maximum observation of 20 m (Khao Lak). An interesting result is that the same match is obtained when considering a homogeneous source (Fig. 4a), although the fault slip is lowered near the latitudes from 5°N to 10°N, and increased northwards.

The absolute values obtained for both models differ, since in the worst case extrapolation to −0.1 m, with the heterogeneous source, the maximum values reach 24 m (Fig. 4b), while in the other case, they do not exceed 20 m (Fig. 4a). For the heterogeneous source, a depth of extrapolation of −1 m allows a better match to the mean values observed in Thailand near the distance of 200 km (x-axis on Fig. 4).

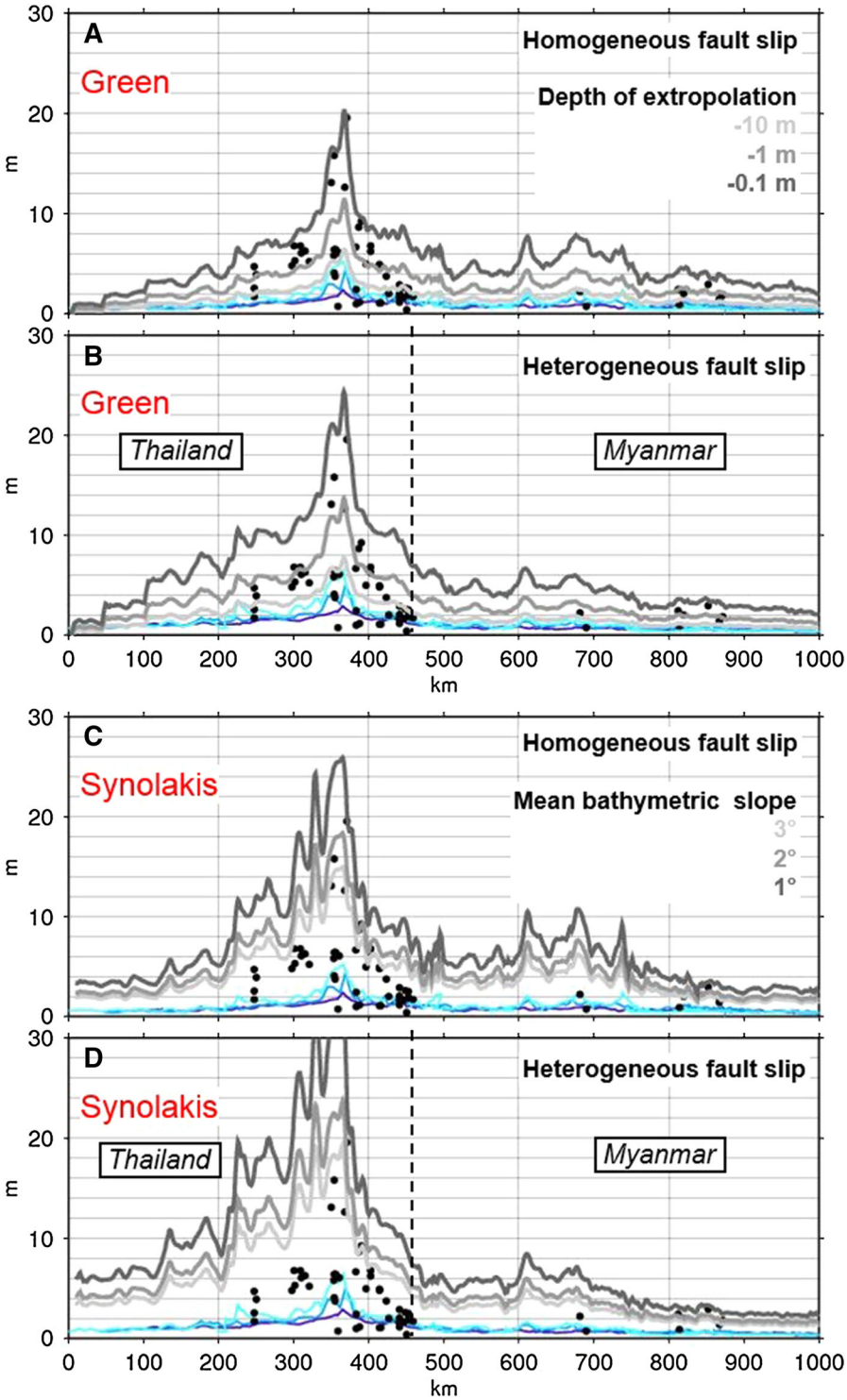

Figure 4

For Thailand and Myanmar, comparison between the measures and the modeling results extrapolated using the Green's law, for the homogeneous (**a**) heterogeneous (**b**) sources, and for the Synolakis law, for the homogeneous (**c**) heterogeneous (**d**) sources. *Colored blue lines* are maximum computed water heights along bathymetric contours of −200 (*dark blue*), −100 (*blue*) and −50 m (*light blue*). Extrapolated values following the Green's law are displayed for depths of extrapolation of −10 m (*light gray*), −1 m (*intermediate gray*) and −0.1 m (*dark gray*). Extrapolated values following the Synolakis law are displayed for the mean bathymetric slopes of 3° (*light gray*), 2° (*intermediate gray*) and 1° (*dark gray*)

In addition, both homogeneous and heterogeneous models display a very interesting trend, underlining the area most exposed for this given source region (Fig. 5). This area, including the Khao Lak and Phuket heavily damaged coastlines in 2004, is clearly identified as a very exposed area for tsunamis coming from this part of the Andaman subduction. This amplification seems to be related to bathymetric features favoring focusing of the tsunami energy at these latitudes, as shown by the maximum tsunami heights computed offshore that appear focused above a submarine ridge directed toward the latitude of Khao Lak (Fig. 5).

4.2.3 *Estimation of Tsunami Heights Using the Synolakis Law*

The main difficulty to apply the law proposed by Synolakis is to estimate the mean submarine slope β. The analysis of the bathymetry used here in the shallow area (<200 m) reveals that the slopes are extremely low for the area off Thailand, not exceeding 1° or 2°.

Contrary to the results using the Green's law, the extrapolations for the various original profiles (taken at $z = -200$, -100 or -50 m) exhibit a significant standard deviation, however, smaller than the one obtained depending on the slope. We computed the average of the 3 results obtained with the 3 deep contours, to concentrate on the variability upon the bathymetric slope. The results (Fig. 4c, d) show that the overall trend is satisfactory using a mean bathymetric slope from 2° to 3°, thus probably exceeding the actual bathymetric slope (as estimated from the grid used coming from ETOPO2). Here again, the heterogeneous model yields higher values than the homogeneous model, due to the higher slip concentrated near latitude 8°N. But as above, the general trend obtained reveals the maximum impacted area, near latitude 9°N.

4.2.4 *Conclusions for the Thailand–Myanmar Case*

We analyzed the 2004 database along the Thailand–Myanmar coastline, and compared it with the first order modeling results performed on a coarse grid. Some remarks can already be made. Even though the parameters estimated for both Green or Synolakis laws may depend on the grid resolution (here 4′), for the Green's law, extrapolations to water depths of 1 m satisfactorily fit the mean observed run-up values, while extrapolations to 0.1 m yield a reasonable distribution for the observed flow depths. The bathymetric slope to consider in the Synolakis law is close to the actual one, actually rather steeper. As for the tsunami

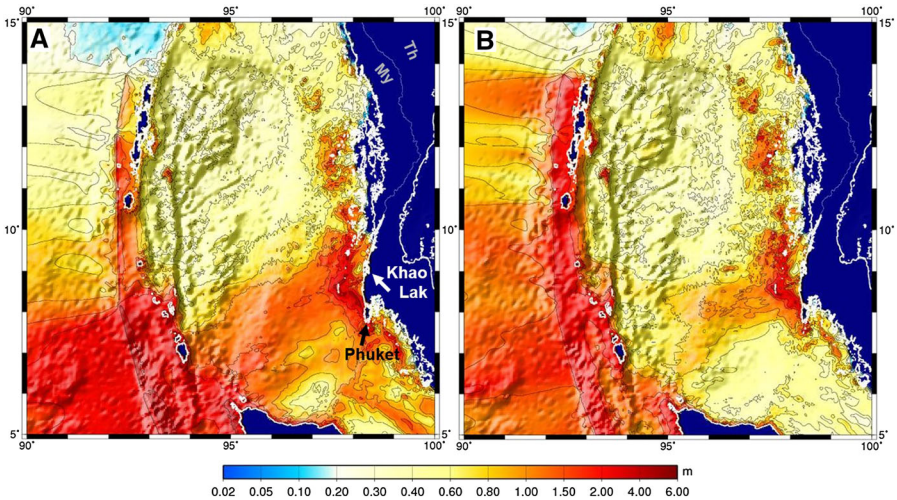

Figure 5
Maximum tsunami heights computed after 4 h of propagation toward Thailand and Myanmar, with the heterogeneous source model (**a**) (*left*) and the homogeneous source model (**b**) (*right*). Note the location of Khao Lak in front of a focusing bathymetric ridge

impact in these areas, the submarine bathymetry off Thailand certainly played a key role in focusing energy toward Phuket and Khao Lak, as was already observed in previous studies (SATAKE *et al.* 2006).

In the following, we will further check whether these parameters obtained for Thailand–Myanmar can also apply to other coastlines, especially at farther distances, using the same earthquake sources and the same coarse modeling. Since numerical dispersion in the numerical modeling may increase the attenuation of computed amplitudes, these parameters may be consequently revised for other coastlines.

4.3. Application to India and Sri Lanka

4.3.1 Observations of the 2004 Tsunami

Observations gathered after the 2004 tsunami, and used here (Fig. 7), consist of run-up values measured along the southeastern coast of India (JAYAKUMAR *et al.* 2005), and of water heights including run-up, around Sri Lanka (LIU *et al.* 2005; GOFF *et al.* 2006). In India, the measures are reported as real run-up values (taken at the inundation limit), and range from 2 to 6 m approximately. In Sri Lanka, only a few run-up measures are available, reaching the maximum values of 9–13 m, while most of the flow depths range from 2 to 6–8 m.

The largest tsunami heights are observed in the southern part of Sri Lanka where a run-up of about 13 m has been reported (Yala region). On the western coastline, the observed tsunami heights are about 4–6 m and can be explained through detailed numerical modeling (POISSON *et al.* 2009).

The maximum water heights computed off India and Sri Lanka (Fig. 6), for the homogeneous source, display two areas of higher impact, the first near latitude 11–12°N, off Pondicherry (Tamil Nadu), and the second off the south of Sri Lanka, near latitude 5°N. These two latitudes are also the places where the impact of the tsunami was the highest. Using the heterogeneous source slightly changes that pattern, lowering the impact near the latitude 11°–12°N, but strengthening the impact to the south of Sri Lanka, corresponding to the reinforced slip in the central part of the earthquake rupture.

4.3.2 Estimation of Tsunami Heights Using the Green's Law

Using the same tsunami modeling results as for the Thailand case, the tsunami heights extrapolated to various sea depths have been computed, for the two earthquake sources considered. When the heterogeneous source model is used, the extrapolated values (Fig. 7b) are higher for the southern Sri Lanka area, in good agreement with the observed trend of the tsunami heights, whereas when the homogeneous model is used (Fig. 7a), the highly impacted area is located to the latitude 12°N, moreover quite in disagreement with the observations. This may also confirm that the slip in the northern extremity of the rupture was not that high as the value chosen for this homogeneous model.

Regarding the absolute values obtained, the depths of extrapolation of −10 and −1 m are sufficient to properly adjust the mean observed trend. This is quite in agreement with the study off Thailand, but rather more pronounced here, since the depth of extrapolation of −0.1 m is clearly overestimating the observed values for Sri Lanka and India. This is even worse for India data, where the extrapolation yields too large values for depths of extrapolation shallower than −10 m. In India, the available data are run-up values only, thus flow depths may have been locally much higher, but no information was available to give more precision. In addition, the coastal feature near latitude 11°N–12°N, which corresponds to a less pronounced and milder slope offshore, with a more concave pattern for the submarine bathymetry, seems to favor modeled tsunami amplification for those latitudes: this is, however, not confirmed by the data available here, which are thus more consistent with a moderate source fault slip near 10°E.

In Sri Lanka, both available observations and our models are consistent with a maximum value in the southern extremity of the island, a rather different pattern than the modeling results obtained in another study where this place appears as less impacted compared to the western and eastern coastlines (POISSON *et al.* 2009). For the western shoreline, it seems that the extrapolation value of 0.1 m better compares well with the modeling performed in the data and detailed results obtained for the southwestern coast of Sri Lanka (POISSON *et al.* 2009).

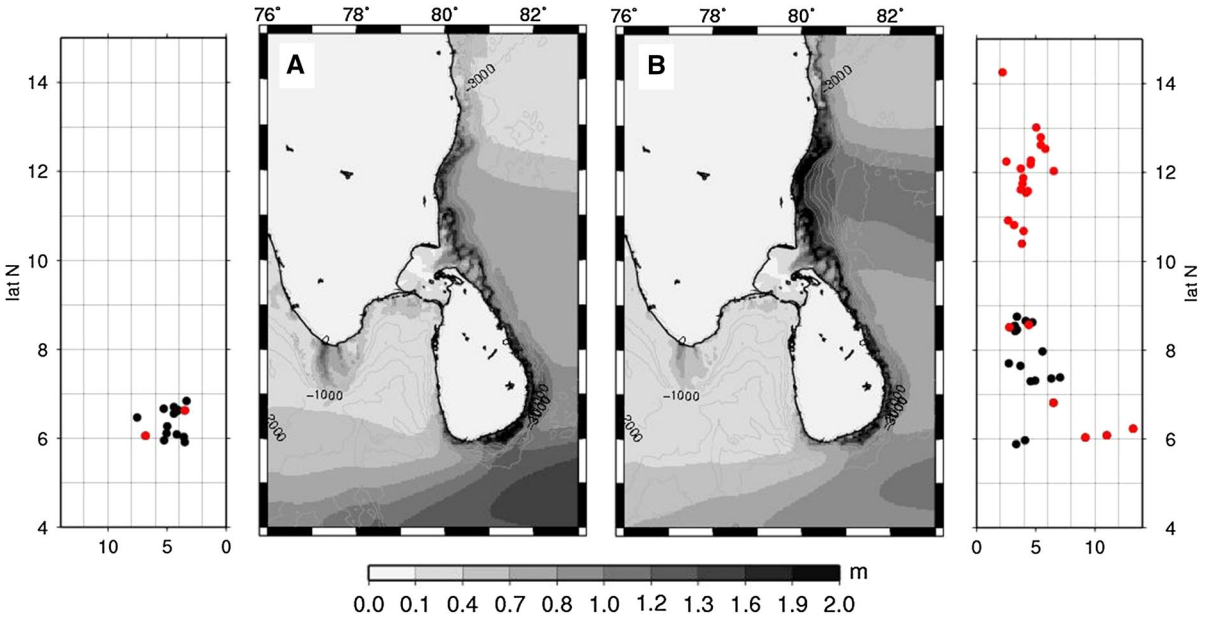

Figure 6
Central panels maximum sea elevations from the heterogeneous (**a**) and homogeneous (**b**) models, after 4 h of propagation, also displaying several annotated bathymetric contours. *Left and right* synthesis of the observations gathered in eastern India (JAYAKUMAR *et al.* 2005) and Sri Lanka (LIU *et al.* 2005) following the 2004 tsunami

4.3.3 *Estimation of Tsunami Heights Using the Synolakis Law*

Using the same mean bathymetric slopes as for the Thailand case study, the extrapolated values (Fig. 7c, d) exhibit a trend very close to the one obtained for the Green's law, again underlining the importance of the source heterogeneity, and stressing the maximum impact in the southern part of Sri Lanka, and off Pondicherry (Tamil Nadu). As in the Thailand case study, the bathymetric slopes requested to better fit the observations should be close to 3° at least.

A more detailed analysis of the bathymetry off Sri Lanka and India reveals that the continental shelf is narrower than off Thailand, and that submarine slopes within the shelf are very low, and very similarly close to 1°–2°. But the border of the submarine shelf is rather steeper and reaches more than 5°–7°, over distances of a few tenths of kilometers. This may explain why a steeper mean slope must be taken into account to better fit the data with the Synolakis law.

4.3.4 *Conclusions for the India–Sri Lanka Case*

The results show that the parameters used to fit data for India and Sri Lanka slightly differ from the ones used for Thailand, since extrapolation depths lower than 1 m are not requested here. As for the Synolakis law, taking into account mean slopes larger than 3° are satisfactory.

The source heterogeneity also plays a more important role than in the Thailand case. This is understandable since the tsunami spreading at distance implies a high dependence on the initial slip latitudinal contrasts, for the kind of distant impacted points studied in Sri Lanka and India. In Thailand, the same source heterogeneities produce less contrasted tsunami heights, all the more as the observed highest values in Thailand are confined within less than 200 km. In Sri Lanka and India, these source heterogeneities imply distinct peaks of amplitude at least 500 km apart, and the heterogeneous model allows to better fit the large observations in south Sri Lanka and the more moderate observations off India.

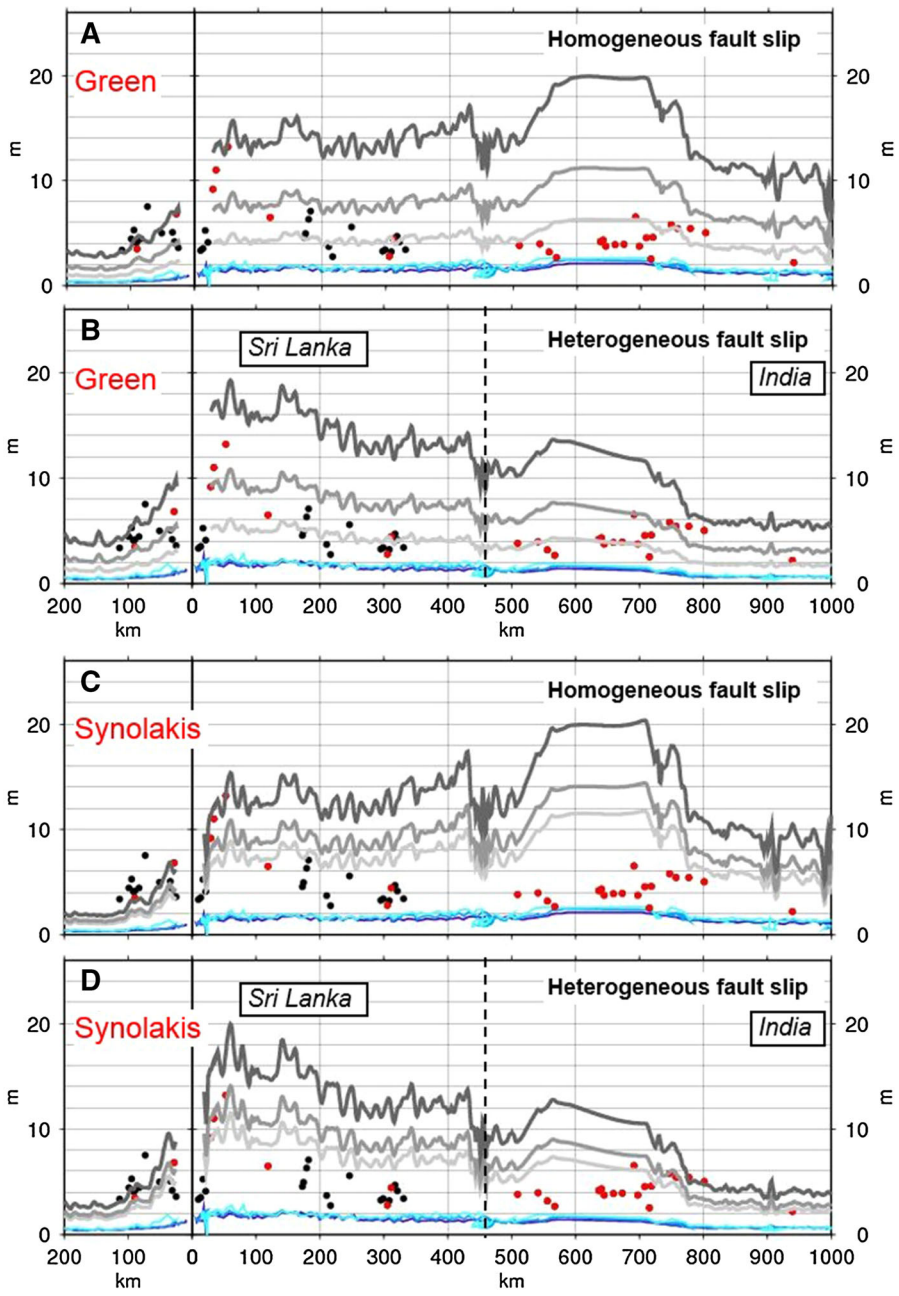

Figure 7

For Sri Lanka and SE India, comparison between the measures and the modeling results extrapolated using the Green's law, for the homogeneous (**a**) heterogeneous (**b**) sources, and for the Synolakis law, for the homogeneous (**c**) heterogeneous (**d**) sources. *Blue* and *gray color scales* as in Fig. 4

4.4. Application to Madagascar

4.4.1 Observations of the 2004 Tsunami

The eastern Madagascar shoreline has been significantly impacted by the 2004 tsunami, with run-up values from 1 to 5 m very locally, but generally comprised between 2 and 3 m (Fig. 8), and with a child drowning to be deplored. Local resonance phenomena led to strong disturbances in the harbor of Toamasina, near latitude 18°S (Okal *et al.* 2006a). While the western shoreline

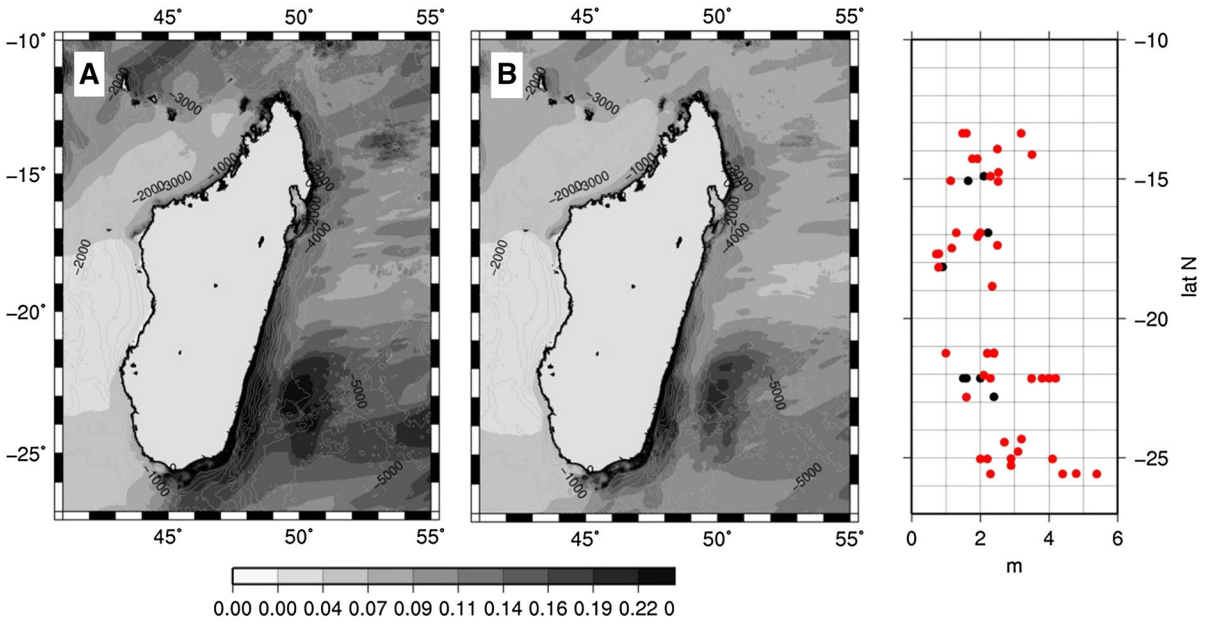

Figure 8
Synthesis of the observations gathered in Madagascar (Okal *et al.* 2006a) following the 2004 tsunami. The *left panel* displays the maximum water heights computed after 10 h of propagation, using the heterogeneous (**a**) and homogeneous (**b**) source models. Run-up values are in *red*, flow depths in *black*

was poorly impacted, some doubts remain on the southernmost shore where local edge waves may have produced damage (Okal *et al.* 2006a).

4.4.2 *Estimation of Tsunami Heights Using the Green's Law*

The homogeneous source model (Fig. 9a) underestimates the maximum tsunami height observations, even for the shallowest depths of extrapolation, by a factor of almost 2. However, the overall trend is well reproduced, underlining the larger tsunami impact along the southeasternmost shoreline. This discrepancy could be discussed with respect to the fact that most of the observations used here are run-up values, contrary to the previously studied sites where they mostly consisted in tsunami flow depths. But above all, the observed absolute values considered in Madagascar (from 2 to 4 m on average) are much lower than the two previously studied sites, thus the obtained results are quite satisfactory as far as the relative ratios are concerned.

Using the heterogeneous model (Fig. 9b) improves the fit by enhancing the computed impact to the South. Only the extreme values to the South cannot be satisfactorily fit. As for La Réunion Island (location on Fig. 1) (Hébert *et al.* 2007), this source is most probably more realistic for these remote targets, because the highest slip off North Sumatra, in the southern central region of the rupture, contributes to more tsunami energy toward this region of the Indian Ocean.

4.4.3 *Estimation of Tsunami Heights Using the Synolakis Law*

Again the same parameters have been applied to study how the Synolakis law can reproduce the overall trend of the 2004 observations in Madagascar. As for the Green's law, the heterogeneous model (Fig. 9d) better fits the observation distribution than the homogeneous source (Fig. 9c), but still the extreme values to the South are not well explained.

Using a very low slope of 1° allows fitting well the observed trend. In this case, the extrapolation must therefore be reinforced. And it is worth noting that the submarine slopes off Madagascar are rather steeper than in the two previous studied areas: south to 20°S, they reach 3°–4°, but north to 20°S a narrow shelf break displays slopes from 5° to 7°. These

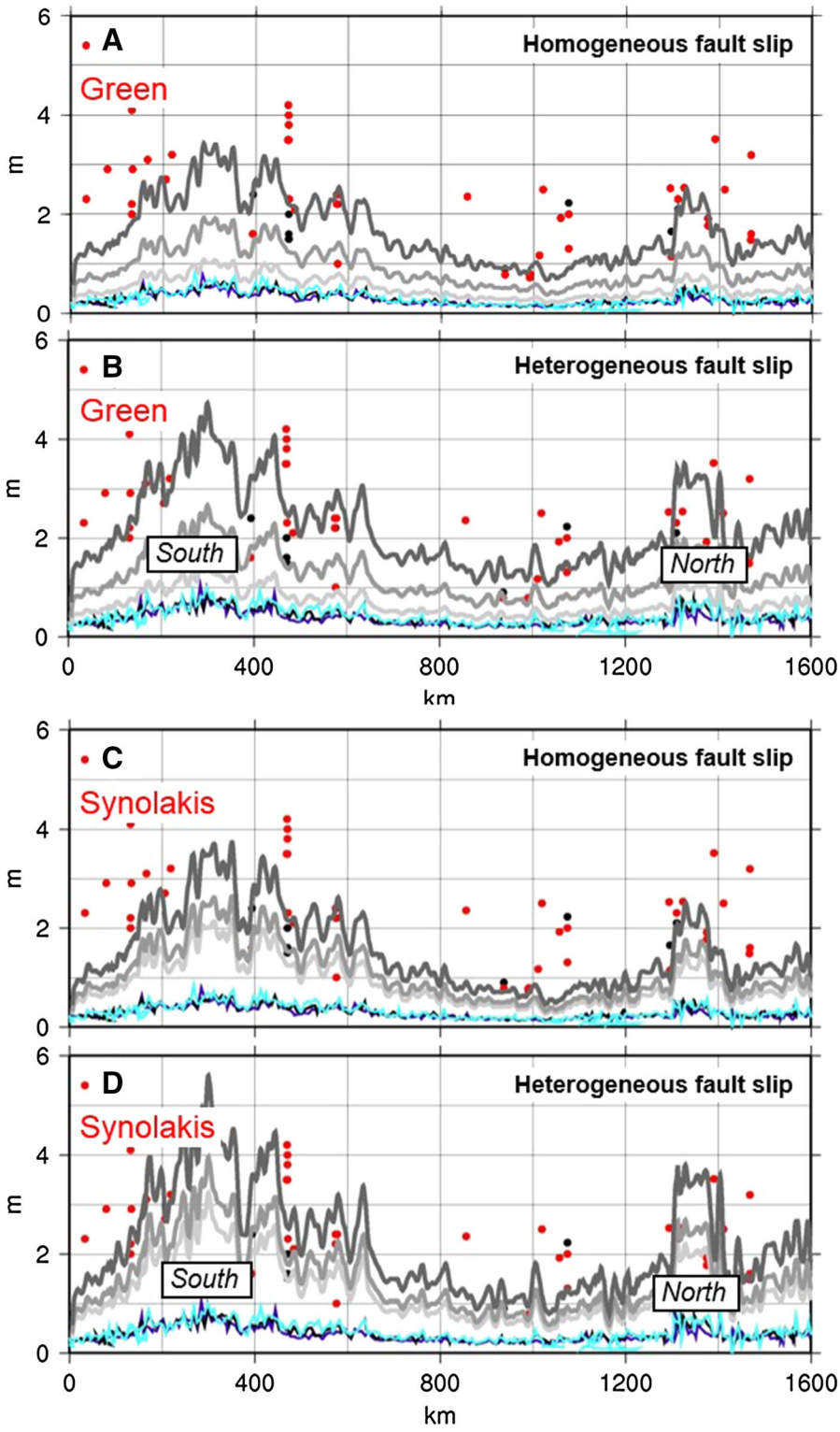

Figure 9
For Madagascar, comparison between the measures and the modeling results extrapolated using the Green's law, for the homogeneous (**a**) heterogeneous (**b**) sources, and for the Synolakis law, for the homogeneous (**c**) heterogeneous (**d**) sources. *Blue and gray color scales* as in Fig. 4

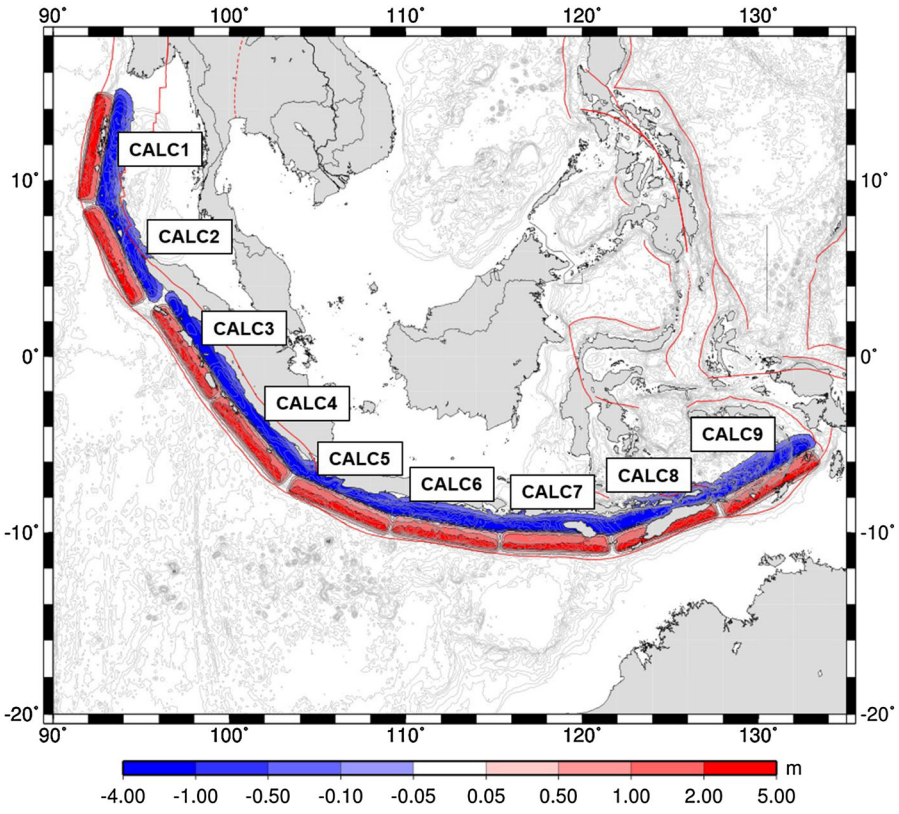

Figure 10
Initial coseismic deformations for the M_w 9.0 earthquakes for the statistical test

contrasting slopes are in good agreement with the contrasting observations in north and south Madagascar, but they also confirm that the extrapolation method is not able to fit the data for such realistic slopes.

4.4.4 *Conclusions for the Madagascar Case*

For both employed methods, the extrapolated models tend to underestimate the observations, especially when the fault slip model is simply homogeneous. Using a heterogeneous model improves the fit, except for the extreme values observed in the southern part of the island.

A reason for the general discrepancies between the extrapolated models and observations may also come from the tsunami model used in this study: at such propagation distances, the numerical dispersion may appear due to the use of coarse grids, and this may have further reduced the computed amplitudes, compared to Thailand and Sri Lanka. Such a bias could also be taken into account. Nevertheless the method reproduces well the relative, overall trend of the data, with larger values to the south than to the north, and with locally higher tsunami heights near latitude 14°S.

5. *Proposition for a Statistical Analysis*

The first aim of this study, discussed in the previous section, was to test amplification laws against actual observations gathered during a specific, well documented event, the 2004 tsunami. A second objective is to study a series of earthquake scenarios to assess the variability of their impact for a given coastline. To this end, we conducted a study based on several scenarios in the Andaman Sea and along the Sumatra–Java trench, using magnitude M_w 9.0 events, larger than the March 2005 earthquake which generated a very weak tsunami (Geist *et al.* 2006).

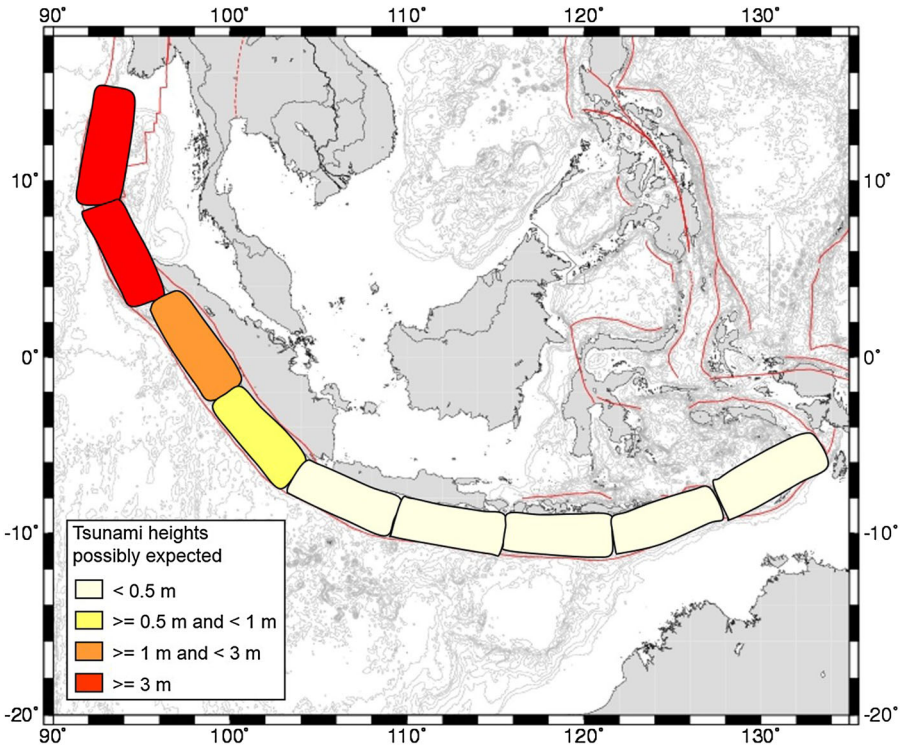

Figure 11
Mapping of the possible tsunami heights to be expected along the Thailand and Myanmar coastline, for the different scenarios

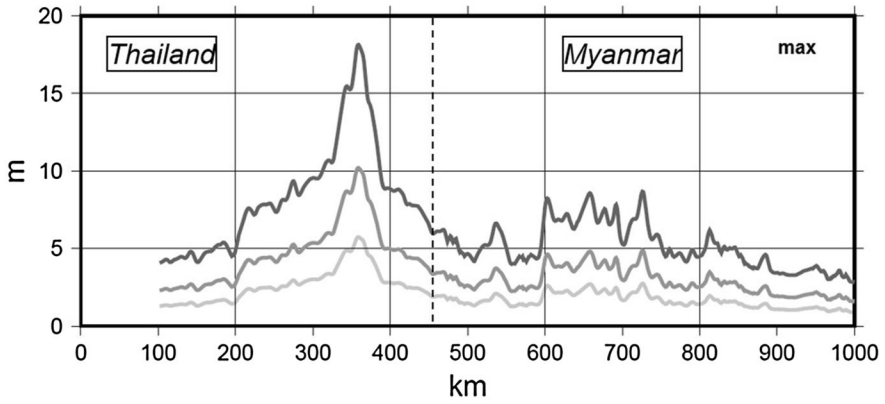

Figure 12
Maximum impact along Myanmar and Thailand, for 4 different M_w 9.0 earthquakes in the Andaman–Sumatra subduction zones, amplified using the Green's law

This level of magnitude is not corresponding to the worst case scenario which could amount to $M_w = 9.3$. Nevertheless, the second largest earthquake that occurred in the last decade is the Tokoku-Oki event on March 11 2011 (Koketsu *et al.* 2011) and it reminds us of the possibility of magnitudes above 9.0 in places where they were not foreseen at all. In addition Zachariasen *et al.* (1999) have suggested that the giant Sumatran subduction earthquake that occurred on November 24 1833 had an 8.8–9.2

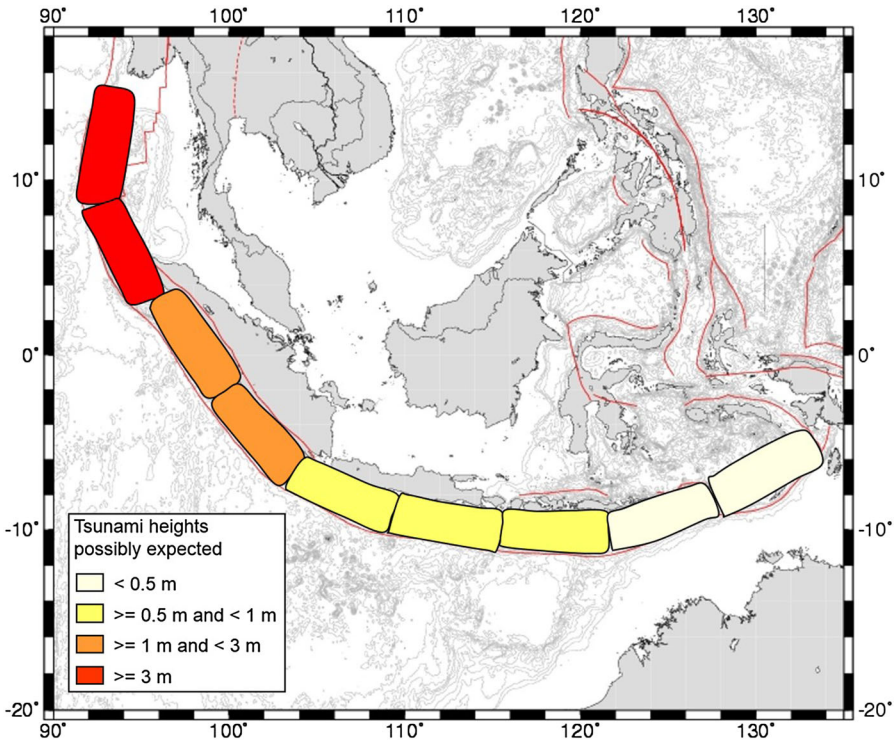

Figure 13
Mapping of the possible tsunami heights to be expected along the SE Sri Lanka and SE India coastlines, for the different scenarios

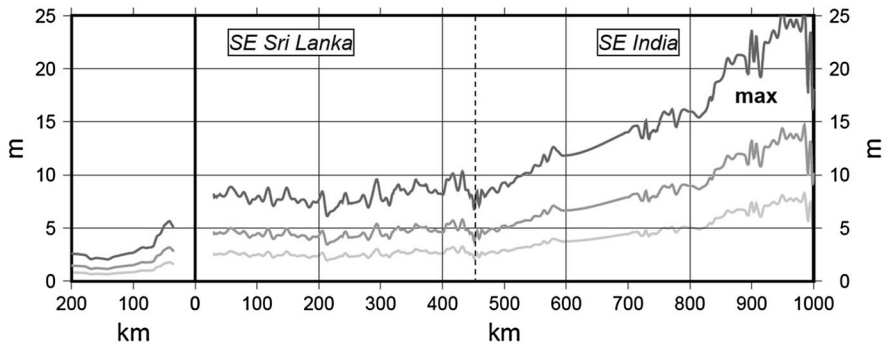

Figure 14
Maximum impact along SE India and Sri Lanka, for 4 different M_w 9.0 earthquakes in the Andaman–Sumatra subduction zones, amplified using the Green's law

M_w magnitude. We considered in this study that a magnitude M_w 9.0 earthquake should be therefore expected all along the Sumatra and Java trenches.

The rectangular sources used are 650 km long and 130 km wide, with a uniform fault slip amounting to 10 m, and an 11° dip angle (Fig. 10). Then the extrapolations have been carried out using the Green's law only.

5.1. The Thailand–Myanmar Case

The estimated impacts can be mapped onto the source areas, in order to represent the variability of the source with respect to the tsunami heights generated, for a given exposed shoreline (Fig. 11). We applied the same extrapolation depths as those previously validated against the 2004 data, i.e. using 0.1–1 m. Obviously this

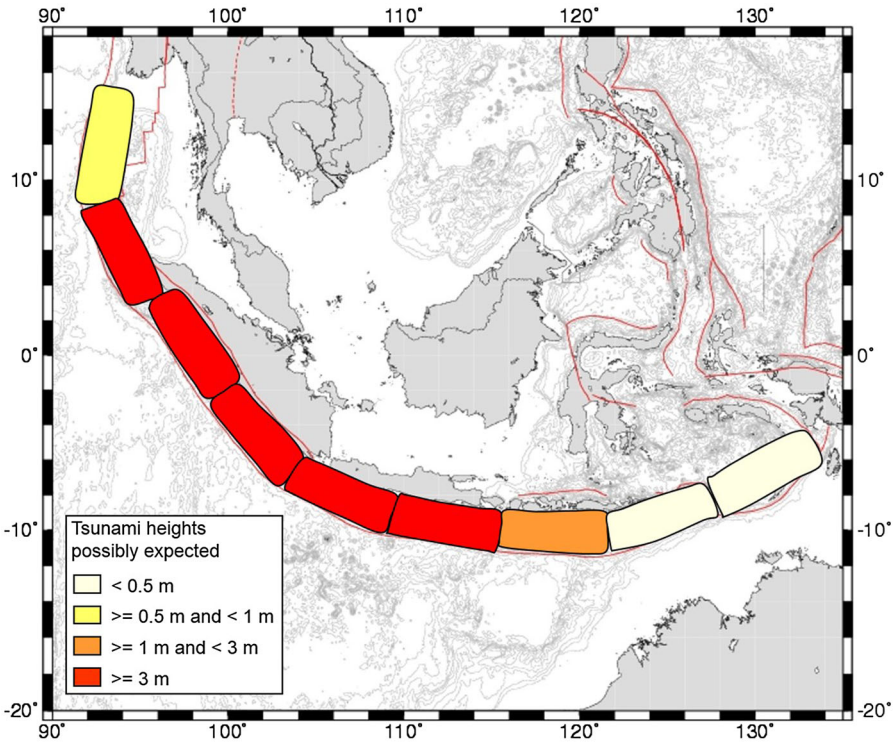

Figure 15
Mapping of the possible tsunami heights to be expected along the Madagascar coastline, for 8 different scenarios

mapping does not provide any information on the variability of the impact along the studied shoreline, but it allows identifying the threatening source areas on average. As expected, none of the sources located southeast to Sumatra produces any impact to Thailand and Myanmar coastlines.

The maximum value of the 4 scenarios exhibits a maximum of 15–18 m near Khao Lak in Thailand (Fig. 12), underlining the important exposure of the area to tsunami hazard, as already observed during the 2004 event (Figs. 4, 5). To a lesser extent the Myanmar coast from the distance 600 to 700 km (x-axis) also offers an important exposure of 7–8 m (near latitude 12°N).

The maximum value along the shoreline stresses again the different behavior of Thailand and Myanmar, mostly due to the bathymetric pattern off these coasts.

5.2. *The India–Sri Lanka Coastline*

Regarding SE India and Sri Lanka, representing the tsunami impacts onto the source map stresses that the most threatening M_w 9.0 sources are located off Andaman and Sumatra (Fig. 13). The sources located south of Java have a very moderate impact (<1 m) and those located further eastwards have no impact.

The maximum values of the scenarios reach 15–25 m and are much higher in SE India, north to latitude 12°N (Fig. 14). In comparison with the 2004 event, the source which contributes most to this amplification is located near the Andaman Islands.

5.3. *The Madagascar Coastline*

This last example (Fig. 15) is more comprehensive because seven different scenarios produce an impact along the studied shoreline. Looking at the distribution along the shoreline (Fig. 16), the most influencing sources are CALC3, CALC4 and CALC5, and yield, for the worst case (CALC5), maximum tsunami heights exceeding 5 m in Madagascar. Both sources CALC4 and CALC5 are located in a similar direction, as seen from Madagascar, and

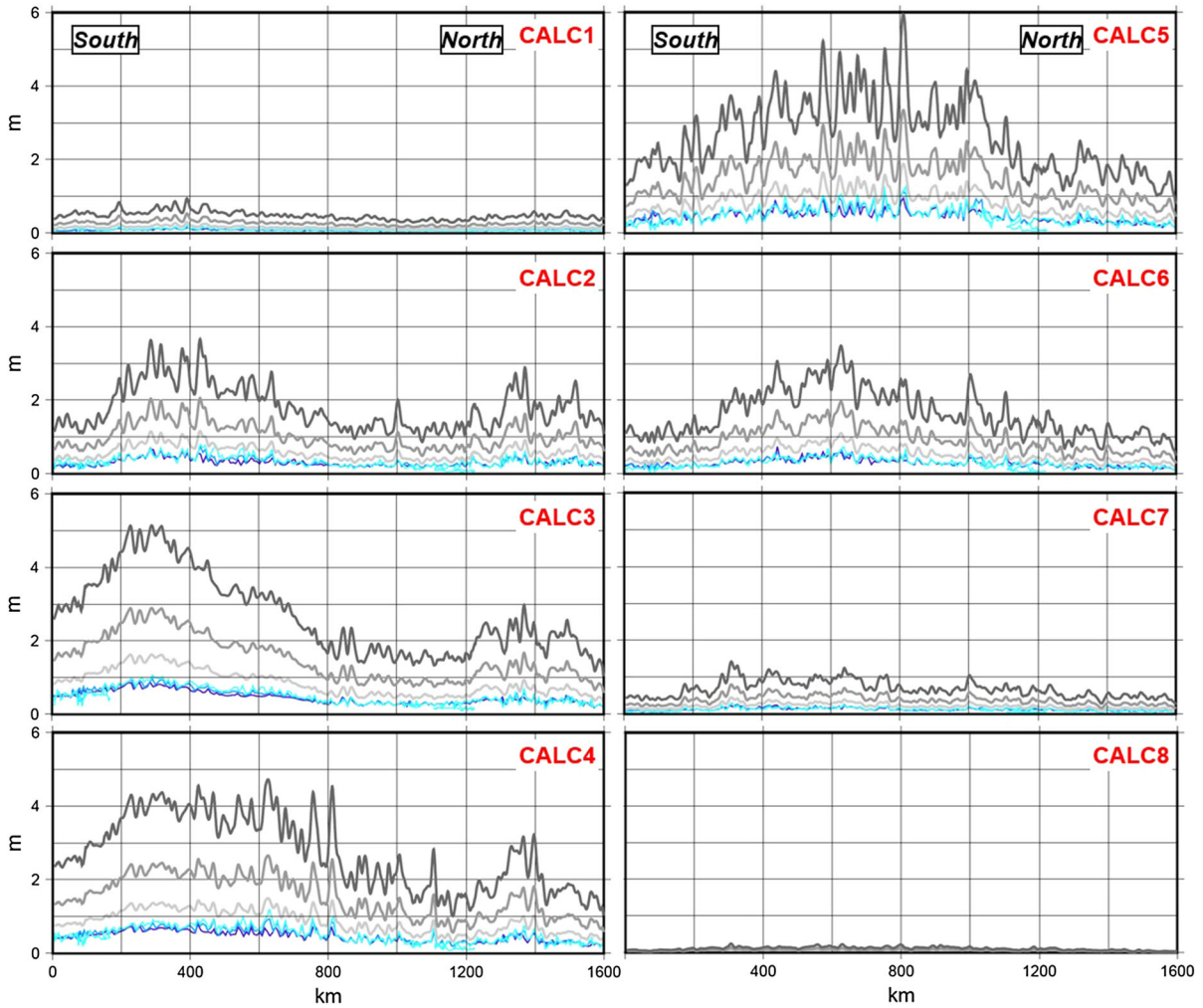

Figure 16
Results of coarse modeling (in *blue*) and extrapolation to various water depths using the Green's law, for the 8 sources studied, and for the Madagascar coastline. The *color codes* are as in Fig. 4 and subsequent

no attenuation of tsunami waves occurs due to archipelagos. The CALC8 and CALC9 sources located to the east do not produce significant heights.

Finally, a preliminary statistical treatment has been applied to all the series obtained from the extrapolations performed with the Green's law (Fig. 17). The idea is to be able to discuss this variability of the impact along a given shoreline. The eight M_w 9.0 scenarios have been used to estimate the 25-th quantile, the median value, the 75-th quantile and the maximum values of the modeled impacts reached along the shoreline. This underlines the more pronounced hazard of South Madagascar with respect to North Madagascar for tsunami sources coming from Sumatra. The median value is lower than 3 m throughout the shoreline, but as the fit using an extrapolation depth of 0.1 m was still underestimating the observations for south Madagascar, this value may be a minimum. 75 % of the scenarios are lower than 4 m, while 25 % of the scenarios are lower than 1.5–2.0 m. The maximum values remind us that the maximum tsunami heights probably range from 5 to 6 m, thus higher than in 2004.

The northern part of Madagascar seems to be more protected from these tsunamis, as in 2004 where the Mascarene Plateau may have played a protective role, and in addition the contrasting mean bathymetric slopes also protect north Madagascar more than

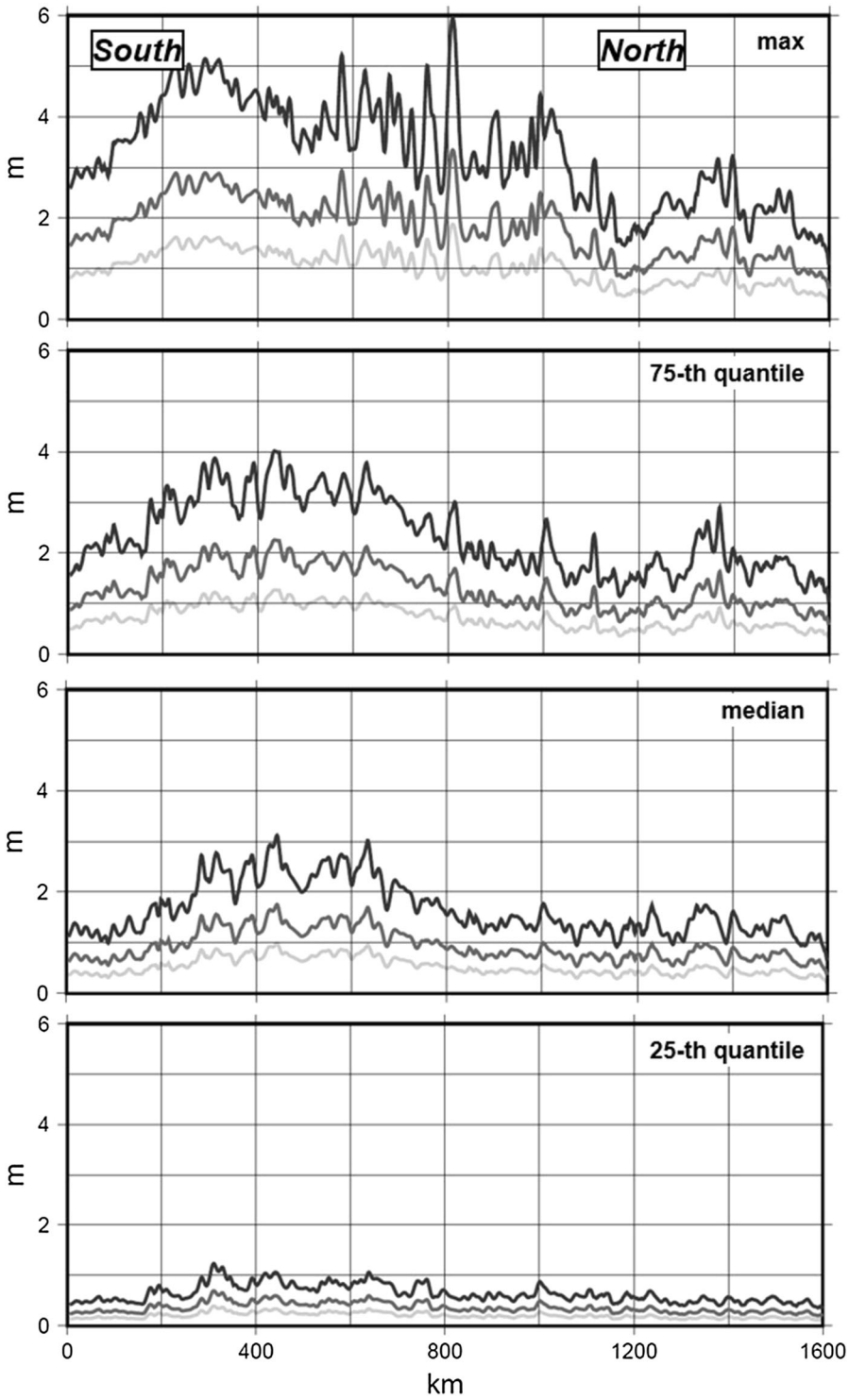

Figure 17
Statistical assessment of the tsunami variability along Madagascar, for 8 different M_w 9.0 earthquakes along the Andaman–Sumatra subduction zone

south Madagascar. However, it is worth noting from the observations in 2004 near latitude 18°S that tsunamis heights from 1 to 2 m can lead to resonance and severe harbor disturbances.

It is also to be mentioned that the magnitude 8.7 March 2005 tsunami (close to, but smaller than the CALC4 used here) was almost unnoticed in Madagascar, possibly because it arrived at night, but also because it was a very weak tsunami (Okal *et al.* 2006a) due a coseismic displacement mainly under islands (Geist *et al.* 2006).

6. Discussion and Conclusions

The analysis of the 2004 tsunami observation databases for 3 selected areas (Thailand–Myanmar, India–Sri Lanka, and Madagascar) has been completed. The distinction between run-up and flow depths must be stressed since the run-up values are not always the maximum values. Using these databases, and modeling results obtained using an offshore low resolution bathymetric grid, from which values are taken along constant depth bathymetric contours, we attempted to fit the observations using either the Green's law or the Synolakis law. The fit is satisfactory in terms of observation variability along the shoreline, and, in many cases, the obtained factor of amplification can be related to particular focusing or defocusing bathymetric features.

Relative higher impacts are well reproduced for some specific sites (Khao Lak, South Madagascar) with respect to other less impacted areas. However, the absolute values are best fit for a set of parameters, mostly similar for all cases in the near field (less than 2 h of propagation), yet slightly different in the far field (Madagascar). This may also be accounted for by the increase of numerical dispersion along with the propagation distance, and thus by a more pronounced spreading for the far field.

When high resolution tsunami models are available, this method can be compared to accurately computed tsunami heights. Most of the amplitudes we obtain with our approach fall well within the range of these highly resolved models, although some specific minimum results in south Sri Lanka are not reproduced here (Poisson *et al.* 2009). Since a similar trend is also observed in other studies (Løvholt *et al.* 2006), probably our model is not accurate enough for the southernmost extremity of Sri Lanka.

Our previous study on La Réunion island could unfortunately not be compared here (Hébert *et al.* 2007) since the 4′ bathymetric grid used was not able to account for the detailed bathymetric features around the island (whose spatial extent does not exceed 40 km). However, we were able to apply the same method to another 300-m grid, and in that case, an extrapolation to 10 to 1-m contours was sufficient to account for the overall distribution of the few observations available (Okal *et al.* 2006b).

Using several scenarios toward the same target, a statistical assessment of the tsunami variability can be proposed, and this was tested more in detail in Madagascar where 8 scenarios can be studied. In this preliminary study, the method allows to map the expected tsunami heights for a given source, or, conversely, to map the overall trend of the expected tsunami heights along the studied shoreline. In brief, the results obtained here underline that:

- Thailand is more exposed to tsunamis than Myanmar. Sources involving M_w 9.0 earthquakes in the Andaman Sea can generally produce tsunami heights much greater than 10–15 m, especially in Thailand, and even more pronounced for the region near Khao Lak, where the submarine morphology seems to contribute to a significant amplification,
- SE India is more exposed than Sri Lanka, with heights greater than 10 m, mostly because of the M_w 9.0 scenario located in the Andaman Sea, but moderate threat from southwards scenarios also exists,
- Madagascar is essentially exposed for its southernmost coasts, where the M_w 9.0 scenarios may produce maximum tsunami heights of 4–6 m.

A statistical assessment has been tried here for Madagascar, which relies on 8 scenarios only, confirming, however, the maximum hazard for South Madagascar. Such an approach could be similarly applied for more numerous, smaller earthquakes to assess tsunami hazard along a given shoreline, for a specific level of magnitude.

Our study also contributes to show some of the uncertainties inherent in the use of amplification laws in the operational context. Indeed, the laws

to be applied should depend on the various parameters influencing the results; hence they have to be defined according to each coastline. Some places are well known to amplify more the tsunamis (for instance, depending on the submarine morphology), and the operational approach should account for these regional conditions (Reymond *et al.* 2012).

Acknowledgments

This work originally benefited from the support of the "Délégation Interministérielle Pour le Tsunami" set up in 2005 by the French Ministry of Foreign Affairs after the catastrophic 2004 Indian Ocean tsunami. It was then supported by the European FP6 TRANSFER project (2006–2009) under the contract 037058. We thank Alberto Armigliato and an anonymous reviewer, as well as the Guest Editor Hermann Fritz, for their valuable comments allowing to improve the quality of the manuscript.

References

Baptista, M.A. and J.M. Miranda, *Revision of the Portuguese catalog of tsunamis* (2009), Nat. Hazards Earth Syst. Sci., *9*, 25–42, www.nat-hazards-earth-syst-sci.net/9/25/2009/.

Baptista, M.A., J.M. Miranda, F. Chierici, and N. Zitellini (2003), *New study of the 1755 earthquake source based on multi-channel seismic survey data and tsunami modeling*, Nat. Hazards Earth Syst. Sci., *3*, 333–340.

Borrero, J.C., Synolakis, C.E., Fritz, H. (2006). *Northern Sumatra field survey after the December 2004 great Sumatra earthquake and Indian Ocean Tsunami*. Earthquake Spectra *22*(S3):S93–S104. doi:10.1193/1.2206793.

Brizuela, B., A. Armigliato, and S. Tinti (2014), *Assessment of tsunami hazards for the Central American Pacific coast from southern Mexico to northern Peru*, Nat. Haz. Earth Syst. Sci., *14*, 1889–1903.

Fujii, Y., and K. Satake (2007), *Tsunami source of 2004 Sumatra-Andaman earthquake inferred from tide-gauges and satellite data*, Bull. Seismol. Soc. Am., *97*, S192–S207. doi:10.1785/0120050613.

Geist, E.L., S.L. Bilek, D. Arcas and V.V. Titov (2006), *Differences in tsunami generation between the December 26, 2004 and March 28, 2005 Sumatra earthquakes*, Earth Planets Space, *58*, 185–193.

Geist, E. L., V. V. Titov, D. Arcas, F. P. Pollitz, and S. L. Bilek (2007), *Implications of the December 26, 2004 Sumatra-Andaman earthquake on tsunami forecast and assessment models for great subduction zone earthquakes*, Bull. Seismol. Soc. Am., *97*, S249–S270. doi:10.1785/0120050619.

GEBCO: The General Bathymetric Chart of the Oceans (2006), http://www.ngdc.noaa.gov/mgg/gebco/gebco.html.

Goff, J., Liu, P.L.-F., Higman, B., Morton, R., Jaffe, B.E., Fernando, H., Lynett, P., Fritz, H., Synolakis, C. (2006). *The December 26th 2004 Indian Ocean tsunami in Sri Lanka*, Earthquake Spectra *22*(S3):S155–S172.

Green G (1837), *On the motion of waves in a variable canal of small depth and width*, Trans. Cambridge Phil. Soc., *6*, 457–462.

Gusiakov, V.K. (2005), *Tsunami generation potential of different tsunamigenic regions in the Pacific, Marine Geology*, *215*, 3–9. doi:10.1016/j.margeo.2004.05.033.

Hébert H., P. Heinrich, F. Schindelé, and A. Piatanesi (2001), *Far-field simulation of tsunami propagation in the Pacific Ocean: impact on the Marquesas Islands (French Polynesia)*, Journal of Geophysical Research, *106*, C5, 9161–9177.

Hébert, H., D. Reymond, Y. Krien, J. Vergoz, F. Schindelé, J. Roger, and A. Loevenbruck (2009), *The 15 August 2007 Peru earthquake and tsunami: influence of the source characteristics on the tsunami heights*, Pure and Applied Geophysics, *166*, 1–2, 211–232.

Hébert, H., A. Sladen, and F. Schindelé (2007), *Numerical modeling of the great 2004 Indian Ocean tsunami: focus on the Mascarene Islands*, Bull. Seismol. Soc. Am., *97*, 1A, S208–S222.

Heinrich, P., F. Schindelé, S. Guibourg and P. Ihmlé (1998), *Modeling of the February 1996 Peruvian tsunami*, Geophys. Res. Lett., *25*, 2687–2690.

IOC (Intergovenmental oceanographic commission) (2013), Tsunami Glossary, Technical Series no. 85.

Ioualalen, M., J. Asavanant, N. Kaewbanjak, S.T. Grilli, J.T. Kirby, and P. Watts (2007), *Modeling the 26 December 2004 Indian Ocean tsunami; case study of impact in Thailand*, J. Geophys. Res., *112*, C07024.

Jankaew, K., B.F. Atwater, Y. Sawai, M. Choowong, T. Charoentitirat, M.E. Martin, A. Prendergast (2008), *Medieval forewarning of the 2004 Indian Ocean tsunami in Thailand*, Nature, *455*, 1228–1231. doi:10.1038/nature07373.

Jayakumar, S. D. Ilangovan, K.A. Naik, R. Gowthaman, G. Tirodkar, G.N. Naik, P. Ganeshan, R.M. Murali, G.S. Michael, M. V. Ramana, G. C. Bhattacharya (2005), *Run-up and inundation limits along southeast coast of India during the 26 December 2004 Indian Ocean tsunami*, Curr. Sci. India, *88*, 11, 1741–1743.

Kanamori, H., and D.L. Anderson (1975), *Theoretical basis of some empirical relations in seismology*, Bull. Seismol. Soc. Am., *65*, 1073–1095.

Koketsu, K., Y. Yokota, N. Nishimura, Y. Yagi, S. Miyazaki, K. Satake, Y. Fujii, H. Miyake, S. Sakai, Y. Yamanaka, T. Okada (2011), *A unified source model for the 2011 Tohoku earthquake*, Earth Planet. Sci. Lett. *310*, 480–487.

Lavigne, F., R. Paris, D. Grancher, P. Wassmer, D. Brunstein, F. Vautier, F. Leone, F. Flohic, B. De Coster, T. Gunawan, C. Gomez, A. Setiawan, R. Cahyadi and Fachrizal (2009), *Reconstruction of Tsunami Inland Propagation on December 26, 2004 in Banda Aceh, Indonesia, through Field Investigations*, Pure and Applied Geophysics, *166*, 1–2, 259–281.

Lorito, S., A. Piatanesi, V. Cannelli, F. Romano, and D. Melini. *Kinematics and source zone properties of the 2004 Sumatra-Andaman earthquake and tsunami: Nonlinear joint inversion of tide gauge, satellite altimetry, and GPS data* (2010), J. Geophys. Res., *115*, B02304. doi:10.1029/2008JB005974.

Løvholt, F., H. Bungum, C.B. Harbitz, S. Glimsdal, C.D. Lindholm, and G. Pedersen (2006), *Earthquake related tsunami hazard along the western coast of Thailand*, Nat. Hazards Earth Syst. Sci., *6*, 979–997. www.nat-hazards-earth-syst-sci.net/6/979/2006/.

Liu, P.L.-F., P. Lynett, H. Fernando, B.E. Jaffe, H. Fritz, B. Higman, R. Morton, J. Goff, and C. Synolakis (2005), *Observations by the International Tsunami Survey Team in Sri Lanka*, Science, *308*, 1595.

Okada, Y. (1985), *Surface deformation due to shear and tensile faults in a halfspace*, Bull. Seismol. Soc. Am., *75*, 1135–1154.

Okal, E.A., H.M. Fritz, R. Raveloson, G. Joelson, P. Pančošková and G. Rambolamanana (2006), *Madagascar Field Survey after the December 2004 Indian Ocean Tsunami*, Earthq. Spectra, *22*, S3, S263–S283.

Okal, E.A., A. Sladen and E.A-S Okal (2006b), *Rodrigues, Mauritius, and Réunion Islands Field Survey after the December 2004 Indian Ocean Tsunami*, Earthq. Spectra, *22*, S3, S241–S261.

Okal, E.A. and C.E. Synolakis (2008), *Far-field tsunami hazard from mega-thrust earthquakes in the Indian Ocean*, Geophys. J. Int, *172*, 995–1015.

Ortiz, M., and R. Bilham (2003), *Source area and rupture parameters of the 31 December 1881 Mw = 7.9 Car Nicobar earthquake estimated from tsunamis recorded in the Bay of Bengal*, J. Geophys. Res., *108*, B4, 2215. doi:10.1029/2002JB001941.

Pelinovsky, E.N., and R. Kh. Mazova (1992), *Exact analytical solutions of nonlinear problems of tsunami wave run-up on slopes with different profiles*, Natural Hazards, *6*, 227–249.

Poisson, B., M. Garcin and R. Pedreros (2009), *The 2004 December 26 Indian Ocean tsunami impact on Sri Lanka: cascade modelling from ocean to city scales*, Geophys. J. Int., *177*, 1080–1090. doi:10.1111/j.1365-246X.2009.04106.x.

Reymond, D., E. A. Okal, H. Hébert, and M. Bourdet (2012), *Rapid forecast of tsunami wave heights from a database of pre-computed simulations, and application during the 2011 Tohoku tsunami in French Polynesia*, Geophys. Res. Lett., *39*, L11603. doi:10.1029/2012GL051640.

Rudloff, A., J. Lauterjung, U. Münch, and S. Tinti (2009), *The GITEWS Project (German-Indonesian Tsunami Early Warning System)*, Nat. Hazards Earth Syst. Sci., *9*, 1381–1382, 2009.

Satake, K., T.T. Aung, Y. Sawai, Y. Okamura, K. S. Win, W. Swe, C. Swe, T.L. Swe, S.T. Tun, M.M. Soe, T.Z. Oo, and S.H. Zaw (2006), *Tsunami heights and damage along the Myanmar coast from the December 2004 Sumatra-Andaman earthquake*, Earth Planets Space, 58, *2*, 243–252.

Sawai, Y., Y. Namegaya, Y. Okamura, K. Satake, and M. Shishikura (2012), *Challenges of anticipating the 2011 Tohoku earthquake and tsunami using coastal geology*, Geophys. Res. Lett., *39*, L21309. doi:10.1029/2012GL053692.

Schindelé, F., A. Gailler, H. Hébert, A. Loevenbruck, E. Gutierrez, A. Monnier, P. Roudil, D. Reymond, and L. Rivera (2015), *Implementation and Challenges of the Tsunami Warning System in the Western Mediterranean*, Pure and Applied Geophysics, *172*, 821–833.

Sladen, A. and H. Hébert (2008), *On the use of satellite altimetry to infer the earthquake rupture characteristics: application to the 2004 Sumatra event*, Geophys. J. Int., *172*, 707–714 doi:10.1111/j.1365-246X.2007.03669.x.

Smith, W.H.F., and D.T. Sandwell (1997), *Global seafloor topography from satellite altimetry and ship depth soundings*, Science, *277*, 1956–1962.

Soloviev, S.L., O.N. Solovieva, C.N. Go, K.S. Kim and N.A. Shchetnikov (2000), Tsunamis in the Mediterranean Sea 2000 BC–2000 AD, Kluwer Academic Publishers, Dordrecht, Netherlands, 243 pp.

Subarya, C., M. Chlieh, L. Prawirodirdjo, J.-P. Avouac, Y. Bock, K. Sieh, A.J. Meltzner, D. H. Natawidjaja, and R. McCaffrey (2006), *Plate-boundary deformation associated with the great Sumatra–Andaman earthquake*, Nature, *440*, 46–51.

Synolakis, C.E. (1991), *Tsunami runup on steep slopes: how good linear theory really is*, Nat Haz., *4*, 221–234.

Synolakis, C. E. (2002), Tsunami and seiche. In Earthquake engineering handbook (ed. W.-F. Chen & C. Scawthorn), pp. 9-1–9-90. New York, NY: CRC Press.

Synolakis, C.E., and E. J. Skjelbreia (1993), *Evolution of maximum amplitude of solitary waves on plane beaches*, J. Water. Harbor Coast. Ocean Eng., *119*, 3, 323–342.

Synolakis, C.E., and Bernard, E.D. (2006), *Tsunami science before and beyond Boxing Day 2004*, Phil. Trans. R. Soc. A, *364*, 2231–2265.

Tadepalli, S, and C.E. Synolakis (1996), *Model for the leading wave of tsunamis*, Phys. Rev. Lett., 77, *10*, 2141–2144.

Tinti, S., A. Armigliato, R. Tonini, A. Maramai and L. Graziani (2005), *Assessing the hazard related to tsunamis of tectonic origin: a hybrid statistical-deterministic method applied to southern Italy coasts*, ISET Journal of Earthquake Technology 42, *4*, 189–201.

Tinti, S., L. Graziani, B. Brizuela, A. Maramai, and S. Galazzi (2012), *Applicability of the Decision Matrix of North Eastern Atlantic, Mediterranean and connected seas Tsunami Warning System to the Italian tsunamis*, Nat. Hazards Earth Syst. Sci., *12*, 843–857.

Tsuji, Y., H. Matsumoto, Y. Namegaya, W. Kanbua, M. Sriwichai, and V. Meesuk (2005), Thailand Tsunami Field Investigation Team, Survey 24 Feb. 4 March 2005. http://www.drs.dpri.kyoto-u.ac.jp/sumatra/thailand2/.

Tsuji, Y., Y. Namegaya, H. Matsumata, S.I. Iwasaki, W. Kanbua, M. Sriwichai, and V. Meesuk (2006), *The 2004 Indian tsunami in Thailand: surveyed run up heights and tide gauge records*, Earth Planets and Space, *58*, 2, 223–232.

Yanasigawa, H., S. Koshimura, K. Goto, T. Miyagi, F. Imamura, A. Ruangrassamee, C. Tanavud (2009), *The reduction effects of mangrove forest on a tsunami based on field surveys at Pakarang Cape, Thailand and numerical analysis*, Estuarine, Coastal and Shelf Science *81*, 27–37. doi:10.1016/j.ecss.2008.10.001.

Zachariasen, J., K. Sieh, F.W. Taylor, R.L. Edwards and W.S Hantoro (1999), *Submergence and uplift associated with the giant 1833 Sumatran subduction earthquake: Evidence from coral microatolls*, J. Geophys. Res., *104*, 895–919.

(Received November 30, 2014, revised June 20, 2015, accepted June 29, 2015, Published online July 24, 2015)